EFFECT OF TEMPERING TEMPERATURE ON MECHANICAL PROPERTIES AND MICROSTRUCTURE OF SINTER HARDENED MATERIALS

by

François Chagnon
Quebec Metal Powders Limited

and

Martin Gagné
Rio Tinto Iron & Titanium Inc.-Technology

ABSTRACT

Sinter hardening enables the production of P/M parts with high strength and apparent hardness after sintering, eliminating the need for a post sintering heat treatment. The availability of sintering furnaces with improved cooling capacity combined with the development of low alloy steel powders specifically designed for sinter hardening make this process particularly attractive for parts that are difficult to quench because of their size and shape. Moreover, the powder mix formulation can be tailored to achieve a particular microstructure. However, because either a partially or fully martensitic structure is obtained after sintering, tempering is usually required to restore the mechanical properties.

A study was carried out to evaluate the effect of tempering temperature on strength, apparent hardness, impact energy and microstructure of specimens made from sinter hardening materials. Test specimens were pressed to 7.0 g/cm^3 from mixes containing 2% copper and the amount of graphite required to reach 0.65 and 0.80% combined carbon. Test pieces were sintered 25 minutes at 1120°C in a nitrogen based atmosphere and cooled at a rate of 0.4°C/s from 650 to 300°C. These were subsequently tempered for 60 minutes at temperatures ranging from 150 to 600°C. The highest tensile strength was reached after tempering at 200°C with values of 1075 and 990 MPa for carbon concentrations of 0.65 and 0.80% respectively. The highest yield strength was achieved at a tempering temperature of 300°C and was related to the transformation of retained austenite into bainite. A second hardening peak due to the precipitation of molybdenum carbides was observed at 500°C for both carbon concentrations.

INTRODUCTION

P/M technology offers a significant advantage over conventional steels to produce near net shape complex parts. Steel powders can be produced over a wide range of compositions by varying the concentrations of alloying elements such as manganese, nickel, molybdenum and chromium. Also, the use of admixed elements makes the production of parts feasible with specific microstructures and mechanical properties. In addition to these factors, the sintering conditions (time, temperature and cooling rate) can be varied to modify the microstructure and the final properties of P/M parts. Sintered parts can be heat treated to further increase strength and apparent hardness. If these are oil quenched, additional cleaning operations before and after quenching are required due to the presence of open porosity which entraps oil and grease [1, 2]. However, by increasing the hardenability of P/M steels, martensitic transformation becomes possible during the cooling phase of the sintering cycle. Although carbon is required to increase the hardenability of steels [3], this element alone cannot enable the transformation of austenite to martensite in existing sintering furnaces. Alloying additions are therefore necessary to further improve the hardenability of the materials and make the hardening of large parts possible [3]. It is generally recognized that for similar alloying additions, a homogeneous microstructure results in improved mechanical properties [4, 5]. This can be achieved via the use of low alloy steel powders or of unalloyed steel powders admixed with elemental additions and processed at a sintering temperature high enough to homogeneously diffuse these elements in the steel matrix [5, 6]. With proper selection of base powders, mix formulations and sintering conditions, sinter hardening enables the production of P/M parts with high strength and apparent hardness in the as-sintered condition [7, 8, 9].

The martensitic transformation is a diffusionless reaction [10], i.e. there is no change in chemical composition but a sudden change in crystal structure as austenite transforms into martensite. Austenite is a face-centered cubic (f.c.c.) structure which changes into a supersaturated solid solution of carbon trapped in a body-centered tetragonal structure by a combination of shearing actions. The degree of distortion increases with the concentration of carbon [10]. Since most sinter hardened materials generally contain a high carbon concentration to ensure high apparent hardness, a tempering treatment is generally required to restore their mechanical properties. The tempering temperature depends on whether the strength or apparent hardness is to be optimized [9]. Since a wide range of microstructures and related mechanical properties can be achieved via sinter hardening, the mechanisms involved during tempering and their effects on the mechanical properties need to be understood. The objective of this study is to characterize the effect of tempering temperature on the mechanical properties and the microstructure of sinter hardened materials.

EXPERIMENTAL PROCEDURE

ATOMET 4701, an Fe-0.45Mn-0.45Cr-1.0Mo-0.9Ni low alloy powder, was used as base material for this study. Two mixes were prepared containing 2% copper and graphite to obtain either 0.65 or 0.80% combined carbon. Specimens of 7.6 cm in length, 1.27 cm in width and 1.11 cm in height were pressed from each mix to a green density of 7.0 g/cm^3 and sintered at 1120°C for 25 minutes in a 90% nitrogen based atmosphere. The cooling rate from 650 to 300°C was 0.4°C/s. Tempering treatments were then carried out at 150, 200, 300, 400, 500, 550 and 600°C for 60 minutes. For temperatures exceeding 200°C, tempering was performed in a nitrogen atmosphere. Specimens were then machined into round tensile and unnotched Charpy test bars according to MPIF Standard 10 and 40 respectively.

Ultimate tensile and yield strengths, elongation, impact energy and apparent hardness were determined by averaging the tests results obtained from six specimens in the as-sintered or tempered conditions. Microstructural characterization was performed by optical and scanning electron microscopy. Retained austenite was determined using x-ray diffraction analysis carried out on polished cross sections of rectangular bars, 1.27 X 1.11 cm^2, mounted in Bakelite. The x-ray scan was carried out using the Cu K_α radiation, λ of 1.540562Å, at a speed of 3 degrees per minute. The x-ray diffraction pattern of Bakelite was identified in order to eliminate its impact on the calculation of the retained austenite.

RESULTS

Results of the mechanical tests are presented in Table 1. It is worth noting that, for both carbon concentrations and all tempering conditions, the specimens exhibited elongation values inferior to 1%. Figure 1 illustrates the effect of tempering temperature on apparent hardness of specimens containing either 0.65 or 0.80% combined carbon. In the as-sintered condition, the highest apparent hardness, i.e. 41HRC is achieved with the high carbon material. This compares to 37 HRC at 0.65% C. Apparent hardness decreases with the tempering temperature to reach, at 400°C, a minimum of 30 and 28 HRC for the 0.80 and 0.65% C contents respectively. It is worth noting that secondary hardening peaks of 36 and 34 HRC were observed when tempering at 500°C for the high and medium carbon levels.

TABLE 1
Apparent hardness, tensile properties and impact energy of specimens containing 0.65 and 0.80% combined carbon tempered at various temperatures (7.0 g/cm³).

C %		As-sintered	Tempering Temperature, °C						
			150	200	300	400	500	550	600
0.65	Apparent Hardness, HRC	37	35	32	29	28	34	30	21
	UTS, MPa	920	1045	1075	1010	925	915	905	895
	YS, MPa	740	750	770	930	875	860	835	820
	Elongation, %	<1	<1	<1	<1	<1	<1	<1	<1
	Impact Energy, J	12	16	19	15	13	12	12	14
0.80	Apparent Hardness, HRC	41	39	37	32	30	36	32	25
	UTS, MPa	815	910	985	945	825	870	910	905
	YS, MPa	690	690	685	880	n.y.	875	850	845
	Elongation, %	<1	<1	<1	<1	<1	<1	<1	<1
	Impact Energy, J	12	17	20	13	12	13	13	13

Figure 2 illustrates the effect of tempering temperature on the ultimate tensile strength (UTS) of specimens containing 0.65 and 0.80% C. Contrary to apparent hardness, the highest UTS values are generally achieved with the 0.65% C material. The tempering treatment significantly increases UTS to reach a maximum at about 200°C for both carbon concentrations, i.e. 1075 and 985 MPa for the 0.65 and 0.80% carbon materials respectively. The UTS then sharply decreases as the tempering temperature increases to 400°C. It is followed by a slower rate of decline for the 0.65%C material and a second UTS peak at 600°C for the 0.80% C one. After tempering at 600°C, both materials exhibit similar UTS values of about 900 MPa.

The effect of tempering temperature on yield strength (YS) is illustrated in Figure 3. Tempering below 200°C does not significantly affect YS for both carbon concentrations. The maximum YS value is however reached at 300°C for both materials. Similar to UTS, the 0.65% C material exhibits the highest YS value. Above 300°C, YS continuously decreases for the 0.65%C material. It is worth noting that for the 0.80% C alloy, no yield was observed when tempering at 400°C. Also, from 500 to 600°C, the high carbon material shows slightly higher YS than the medium carbon material.

Figure 4 presents the effect of tempering temperature on impact energy for the materials containing 0.65 and 0.80% combined carbon. In the as-sintered condition, both materials exhibit impact energy of about 11.5 joules. Tempering significantly increases impact resistance to a maximum of 19 to 20 joules, the 0.80%C materials showing the highest value. Impact energy subsequently declines to a minimum of 12 to 13 joules at 400 to 500°C and is followed by a slight increase in the 500-600°C range.

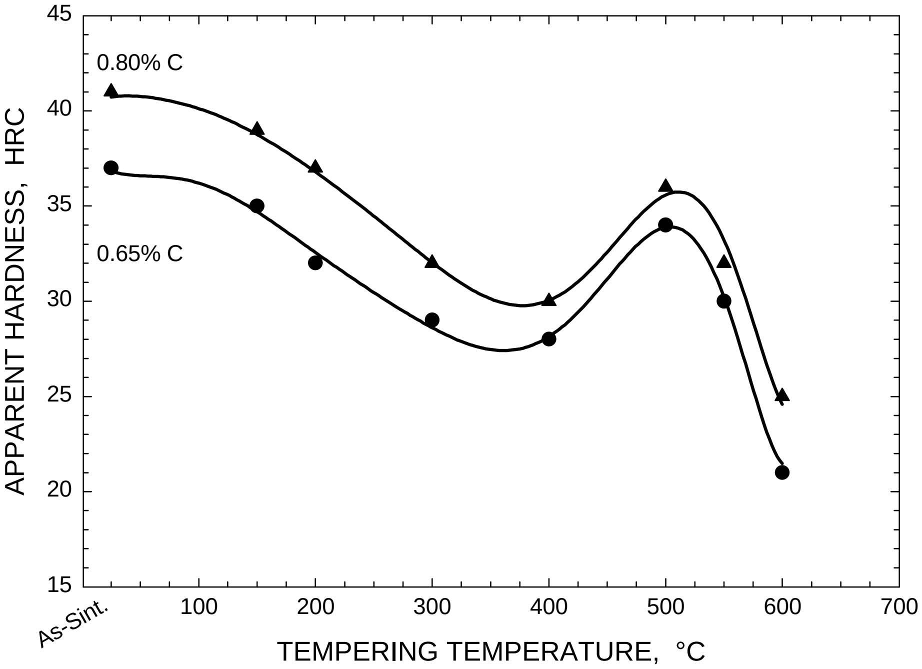

Figure 1. Effect of tempering temperature and carbon content on apparent hardness (ATOMET 4701+C+2% Cu; 7.0 g/cm³).

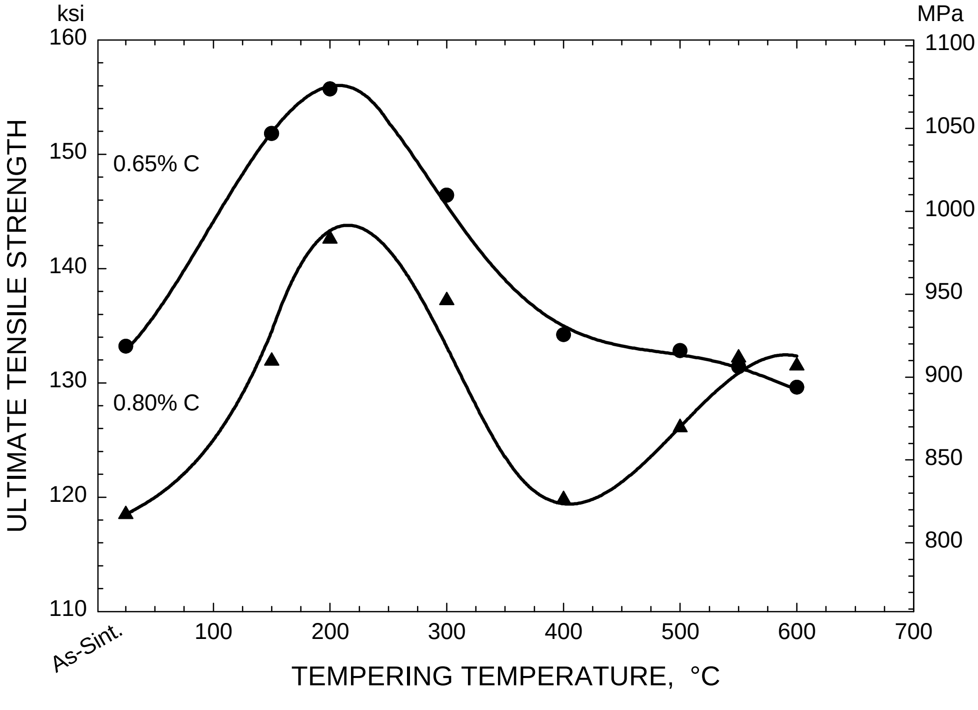

Figure 2. Effect of tempering temperature and carbon content on ultimate tensile strength (ATOMET 4701+C+2% Cu; 7.0 g/cm³).

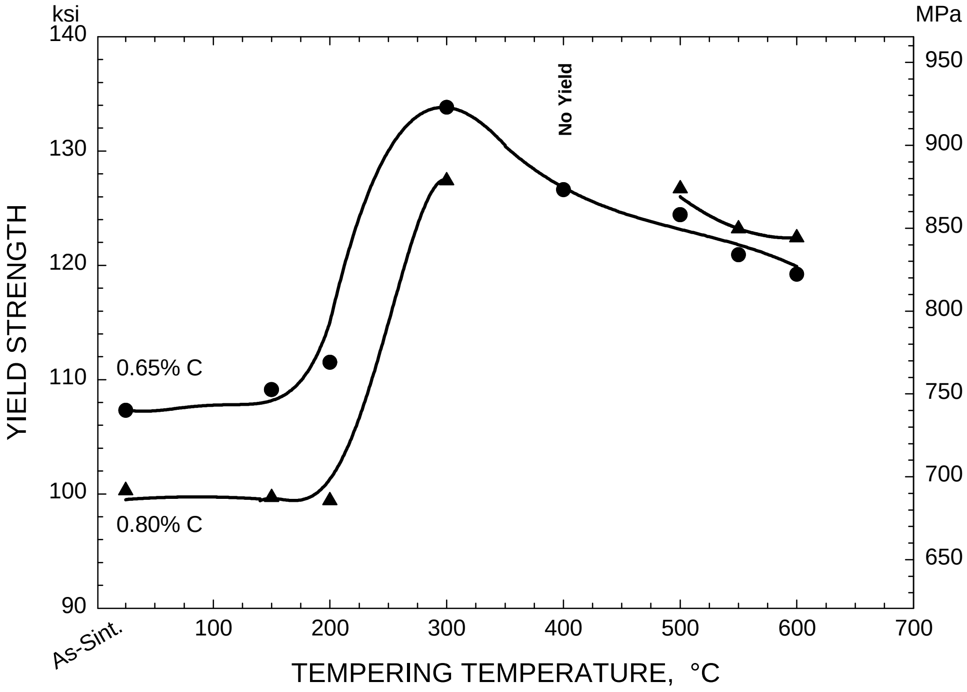

Figure 3. Effect of tempering temperature and carbon content on yield strength (ATOMET 4701+C+2% Cu; 7.0 g/cm³).

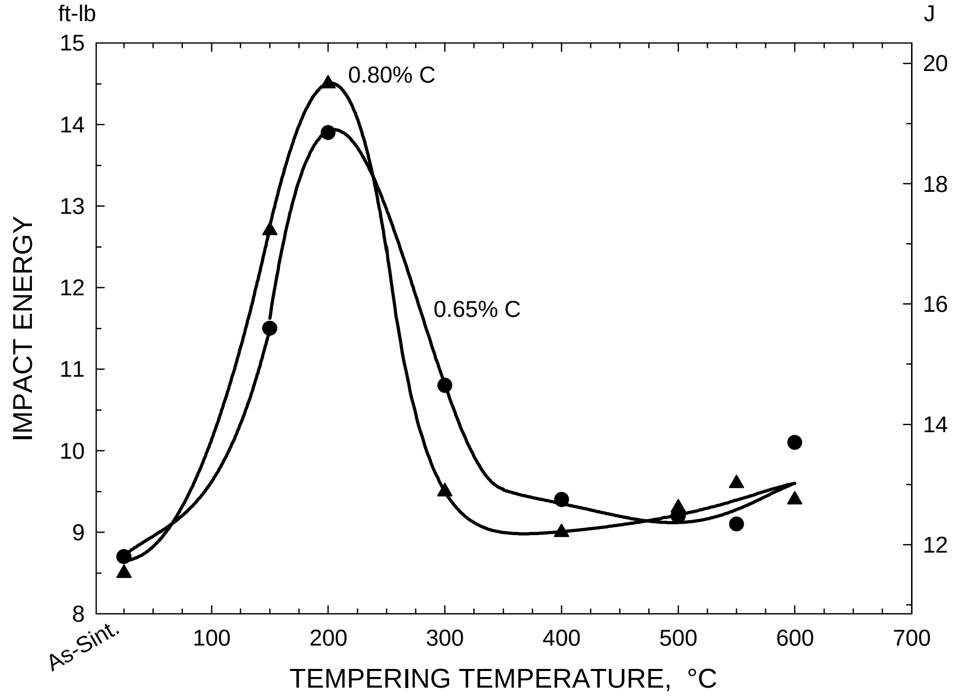

Figure 4. Effect of tempering temperature and carbon content on impact energy (ATOMET 4701+C+2% Cu; 7.0 g/cm³).

DISCUSSION

MICROSTRUCTURE

For both carbon concentrations, sinter hardened materials typically exhibit higher apparent hardness but lower strength and impact energy in the as-sintered condition as compared to after tempering. As illustrated in Figure 5, the microstructure of both materials is mainly composed of martensite with bainite areas which are more abundant in the 0.65% C material. The transformation of austenite into martensite is a diffusionless reaction that takes place only during cooling [10]. The reaction starts at a critical temperature, M_s, which is affected by the carbon content and the concentration of other alloying elements. Increasing the carbon content significantly lowers the critical temperature [10] as well as alloying with elements such as manganese, chromium, molybdenum and nickel. The end temperature of the martensitic transformation, M_f, is not clearly defined since a certain amount of austenite is retained in the structure even at very low temperature, but this temperature drops rapidly as the concentration of carbon and the other alloying elements increases. Austenite is a face-centered cubic (f.c.c.) structure. Because the transformation of austenite to martensite is athermal, there is insufficient time for carbon to diffuse out of solution and the resultant structure is a supersaturated solid solution of carbon entrapped in a body-centered tetragonal structure. This distorted lattice accounts for the high hardness of the martensite but the volume expansion resulting from the martensite transformation induces localized stresses. It is also worth noting from the microstructural observations that the 0.80% C material seems to contain a larger concentration of retained austenite than the 0.65%C material. This was confirmed by the x-ray diffraction analysis carried out on both materials as shown in Figure 6. The 0.85% C material shows a concentration of retained austenite of 28% after sinter hardening. This value is significantly higher than the concentration of 15% measured in the material containing 0.65% C. Tempering at temperatures up to 200°C marginally influences the amount of retained austenite. However, a rapid decrease in the amount of retained austenite is seen as the tempering temperature reaches about 300°C at which its concentration drops to 8% for the high carbon material and to less than 1% for the medium carbon material. At 400°C, there is no retained austenite in either materials. This is well illustrated in Figure 7 for the 0.80% C material. Retained austenite is often located in the vicinity of the pores because of the higher copper concentration found in these areas [12]. There is no significant difference in the microstructure of specimens tempered at 150°C as compared to that of the as-sintered specimens. Below 200°C, the martensite begins to lose its tetragonal structure by forming a hexagonal close-pack transition carbide, ε carbide ($Fe_{2\text{-}3}C$), and low carbon martensite [13]. Above 200°C, two phase transformation phenomena occur; first retained austenite transforms into ferrite and carbides. These are small precipitates in the white zones in Figures 7c and 7d. This is more evident at higher magnification, Figure 8. This fine structure is believed to be bainite as decomposition of retained austenite into bainite generally occurs in the 200 to 300°C range for medium to high carbon steels [14]. The transformation of retained austenite during tempering occurs only after the formation of the transition carbide is well established; the transformation rate of austenite for given temperature and time is then controlled by the diffusion of carbon in austenite [15]. Secondly, the martensite decomposes into ferrite and carbides. In the temperature range of 200 to 300°C, the constituents in high carbon steels are metastable carbides with a composition between those of ε carbides ($Fe_{2\text{-}3}C$) and cementite (Fe_3C) [14]. Above 300°C, cementite (Fe_3C) is the predominant phase. Finally, in the 400 to 600°C range, carbides coalesce to form spheroidite.

RELATIONSHIP BETWEEN MECHANICAL PROPERTIES AND MICROSTRUCTURE

In the as-sintered condition, the material containing 0.80% C shows an apparent hardness four HRC points higher than the material with 0.65% C, despite its higher concentration of retained austenite. The greater lattice distortion resulting from the increase in carbon content overcomes the softening effect of retained austenite. For conventional carbon steels, Figure 9, the hardness of martensite rapidly increases with the carbon content to reach 60 HRC at about 0.4%C. Beyond this concentration of carbon, the rate of increase is significantly reduced up to about 0.80%C to reach 65 HRC and then levels off due to the greater tendency to retain austenite in high carbon steels [16]. A decrease of hardness may appear in steels containing more than 1% C caused by the higher concentration of retained austenite.

Tempering at 150°C results in a slight reduction of apparent hardness by about 2 HRC for both carbon concentrations because the softening effect due to the depletion of carbon from the martensite matrix is compensated by the precipitation of well dispersed small transition carbides. From 150 to 300°C, the rate of reduction of apparent hardness markedly increases because of the softening of the matrix as the martensite looses its tetragonal crystal structure with the precipitation of carbides. However, alloying elements such as molybdenum and chromium, which are strong carbide formers, retard the rate of softening caused by the rapid coarsening of cementite as the tempering temperature is raised. It is worth noting that the transformation of retained austenite into bainite did not affect the rate of reduction in hardness because the difference in apparent hardness between the 0.65 and 0.80% materials is similar to that observed in the as-sintered condition.

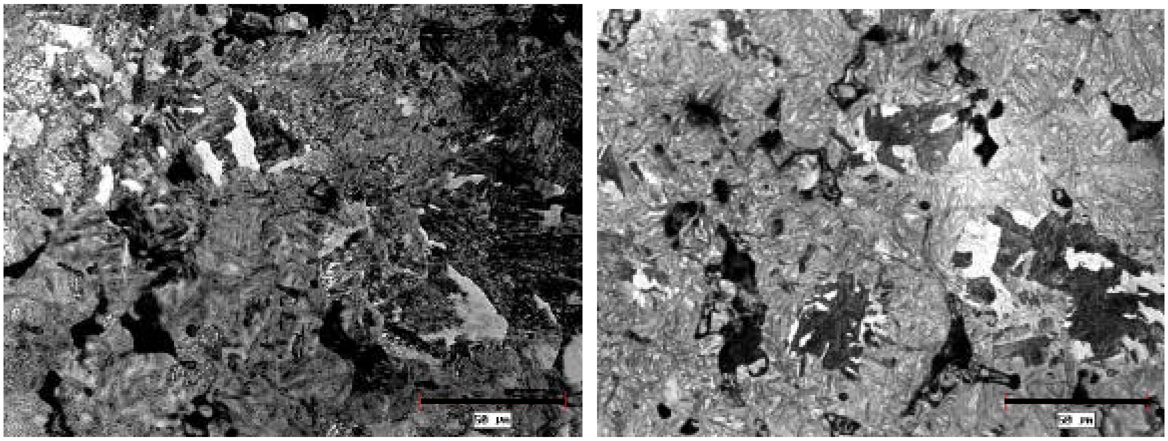

a) 0.65%C b) 0.80%C

Figure 5. Typical microstructure of sinter hardened materials containing 2% copper and 0.65 or 0.80% combined carbon at 7.0 g/cm³.

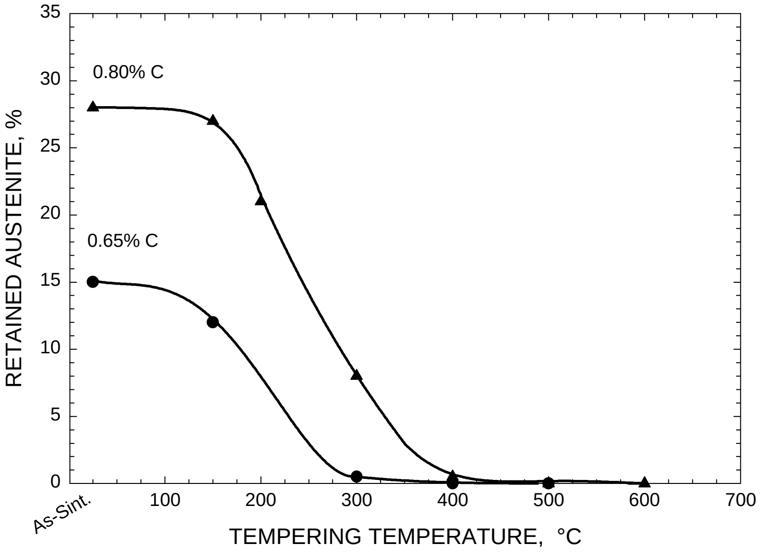

Figure 6. Effect of tempering temperature and carbon content on the transformation of retained austenite (ATOMET 4701+C+2% Cu; 7.0 g/cm³).

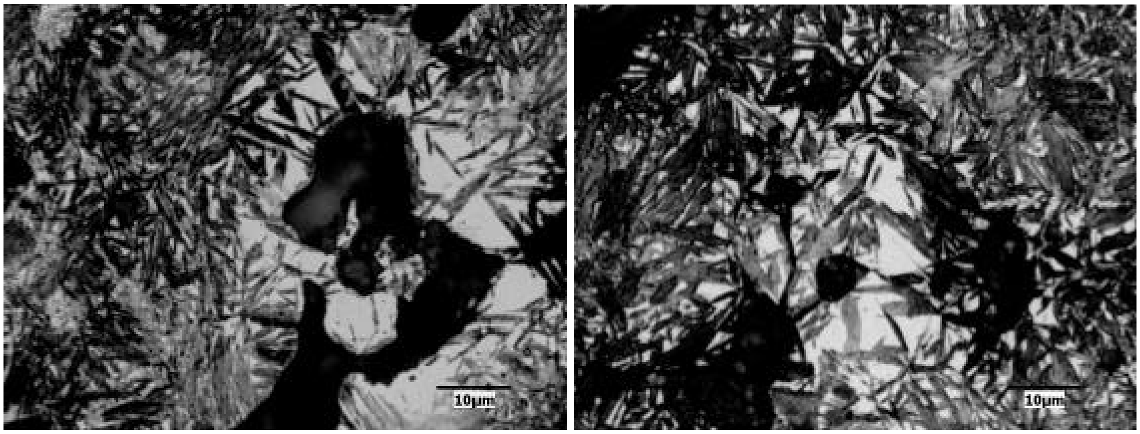

a) As-sintered b) 150°C

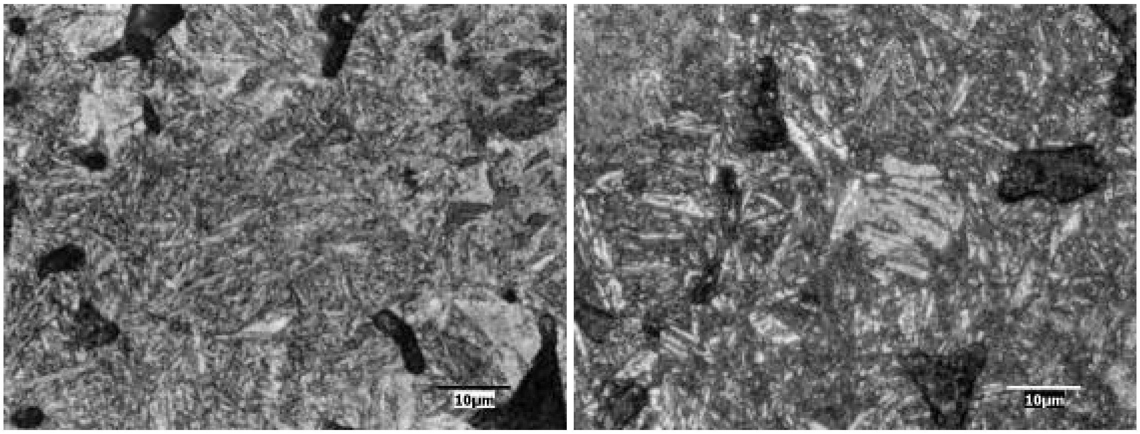

c) 300°C d) 600°C

Figure 7. Evolution of microstructure in sinter hardened specimens containing 2% Cu and 0.80% combined carbon at 7.0 g/cm³ after sintering and tempering at 150, 300 and 600°C.

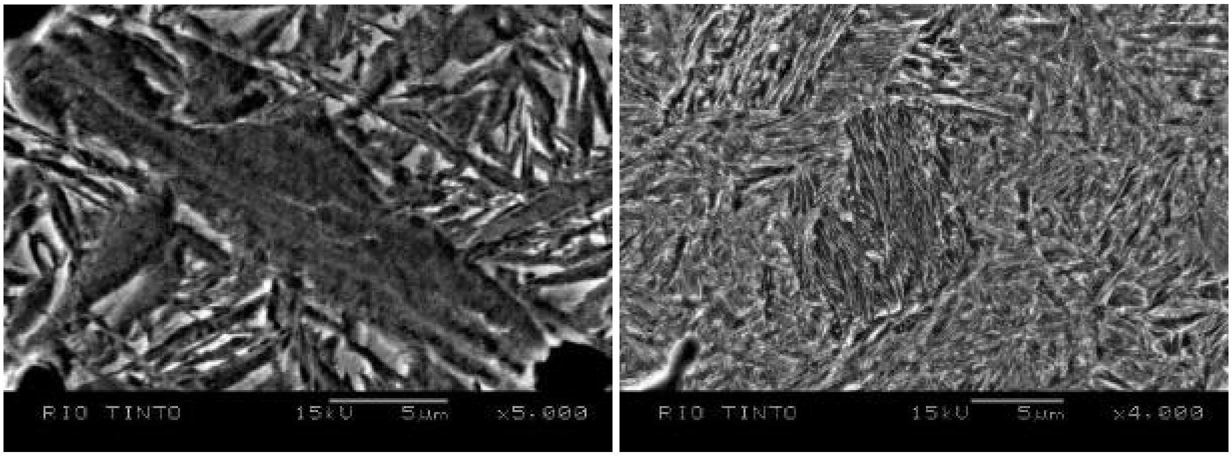

a) 200°C b) 300°C

Figure 8. Effect of tempering temperature on transformation of retained austenite to bainite for specimens containing 0.80%C (tempering time of 60 minutes).

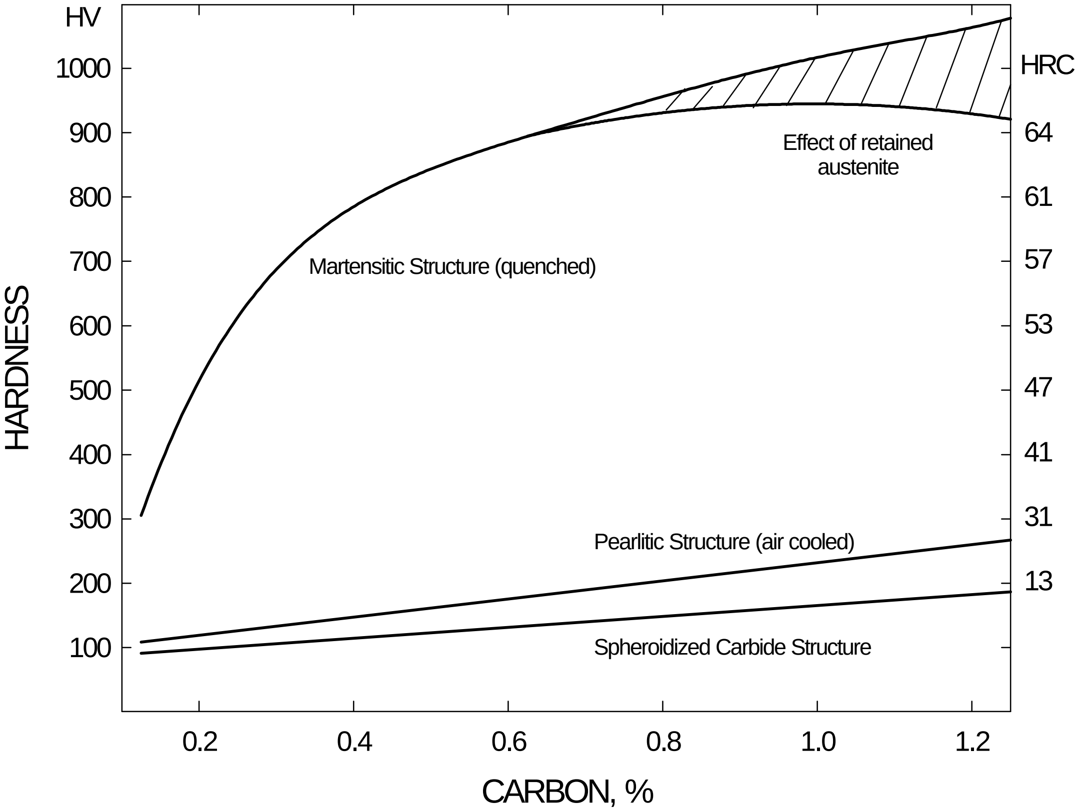

Figure 9. Hardness as a function of carbon content and microstructure in steels [16].

Another important point in Figure 1 is that contrary to plain carbon steels, which show a continuous reduction of hardness with increasing tempering temperature [15], a secondary hardening peak is observed at 500°C. An increase in apparent hardness of 6 HRC is observed for both carbon concentrations as the tempering temperature reaches 500°C. This secondary hardening phenomena is caused by the formation of very fine molybdenum carbides throughout the ferrite matrix [15]. These carbides are known to be especially resistant to coarsening and prevent the softening of the matrix.

Martensite is a hard but very brittle structure. Its brittleness is due to many factors which include lattice distortion, impurity segregation at austenite grain boundaries, carbide formation during cooling and residual stresses induced during quenching [15]. A tempering treatment is thus carried out to reduce brittleness and increase toughness of quenched steels. For sinter hardened materials, residual stresses due to quenching are significantly reduced due to a slower cooling rate but the highly distorted lattice caused by the martensite formation has a negative impact on UTS as seen in Figure 2. The decrease in brittleness due to the relaxation of residual stresses and the precipitation of fine transition carbides allows the sinter hardened materials to reach their optimal strength after tempering at 200°C for both carbon concentrations. The lower UTS values observed with the 0.80%C material for tempering temperatures below 500°C could be related to the effect of alloying elements on the stability and the transformation of the phases on cooling from the sintering temperature. Elements like Ni, Mn, Cr and more particularly Mo shift the eutectoid transformation of steels to lower carbon concentrations as illustrated in Figure 10 [17]. For the base powder used in this study, the carbon content of the eutectoid point is estimated at about 0.40%. The 0.80%C material is therefore largely hypereutectoid. Since the solubility of carbon in austenite is reduced, it is believed that cementite grains nucleate and grow along the austenite grain boundaries because the post-sintering cooling is not fast enough to prevent such nucleation. This affects the cohesion of the former austenite grain boundaries and locally reduces the strength of the materials due to carbon depletion in surrounding regions. This is supported by the temper embrittlement phenomenon observed in the 0.80%C material at 400°C which was not observed with the 0.65%C material because the lower carbon content is closer to the eutectoid point of this alloy. Also, the formation of fine molybdenum carbides in the 500-600°C range strengthens the ferrite matrix. This explains why the rate of reduction of UTS is significantly reduced or almost eliminated for the 0.65%C material. For the 0.80%C material, it is believed that the larger number of fine molybdenum carbides which have precipitated causes the secondary UTS peak observed at 550-600°C range. At that temperature range, both materials exhibit similar UTS.

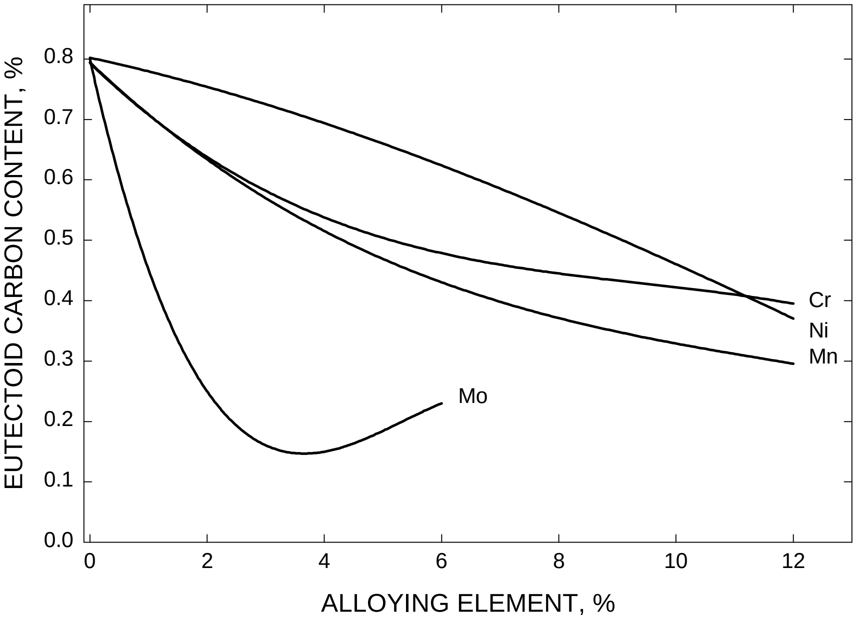

Figure 10. Effect of Cr, Ni, Mn and Mo concentrations on the carbon content of the eutectoid point [17].

Tempering below 200°C does not significantly affect YS, Figure 3. Even if transition carbides precipitate and increase UTS, these do not affect YS. In a composite structure, initial yielding occurs within the weakest phase, which is retained austenite in both materials. It is believed that YS remains unchanged until a significant amount of retained austenite is transformed. This happens as the tempering temperature reaches 300°C where the retained austenite drops to less than 4% for both materials. The highest YS is obtained at this tempering temperature for both materials. Above 300°C, YS slowly decreases due to the transformation of transition carbides into cementite particles which continuously grow in the ferritic matrix. The absence of yield in the 0.80% C material observed at 400°C is probably caused by temper embrittlement as previously discussed. The slightly higher YS observed for the 0.80% C material for tempering temperatures above 500°C is believed to be related to the precipitation of molybdenum carbides, which are presumably more prevalent at this carbon concentration.

In the as-sintered condition, both materials show comparable low impact resistance, Figure 4. Tempering at 150 and 200°C significantly improved impact energy values of both materials but this effect was stronger in the 0.8% C material. This is believed to be related to the stress relief that occurs as the crystal lattice looses its tetragonality and to the presence of a higher amount of retained austenite in this material. After tempering at 300°C, i.e. after the retained austenite is almost completely transformed, the higher carbon material exhibits a lower impact resistance relative to the 0.65% C material. Again, temper embrittlement explains the low values observed for both materials. Finally, as opposed to conventional steels, tempering above 500°C only slightly improves impact resistance of sinter hardened materials.

CONCLUSIONS

Within the range of tempering temperatures, up to 600°C, and carbon concentrations, 0.65 and 0.80%, of this study, it was observed that:

1. The 0.80% combined carbon material showed the highest apparent hardness in both the as-sintered and tempered conditions. Tempering in the 200-400°C range significantly reduced apparent hardness due to the formation of cementite. A secondary hardening peak related to the precipitation of molybdenum carbide was observed at 500°C. Further increase of the tempering temperature significantly reduced apparent hardness due to the growth of the cementite particles.

2. At 0.65% C , the material exhibited higher strength than at 0.80% C for both the as-sintered condition and after tempering up to 500°C. As-sintered, both materials showed low UTS because of the brittleness of un-tempered martensite. Maximum UTS was observed after tempering at 200°C with values of 1075 and 985 MPa for the 0.65 and 0.80% C materials respectively. Temper embrittlement caused a sharp drop of UTS after tempering at 400°C. The precipitation of fine molybdenum carbides in the 500-600°C range was responsible for the plateau of UTS for the 0.65% C material and for the second peak seen on the UTS curve of the 0.80% C material.

3. Higher YS was observed with the 0.65% C material in the as-sintered condition and after tempering up to 300°C. YS was not significantly affected by tempering at 150 and 200°C due to the high concentration of retained austenite. The highest YS for both materials was measured after tempering at 300°C because of complete transformation of retained austenite into bainite. No yield was observed with the 0.80% C material at 400°C due to temper embrittlement. Greater YS values were observed with the higher carbon concentration when tempering above 500°C.

4. Both materials presented similar low impact resistance in the as-sintered condition. The highest impact energy values were obtained after tempering at 200°C for both carbon contents, with the 0.80%C material showing the highest impact energy. This is believed to be related to the larger amount of retained austenite in this material. Temper embrittlement was also observed at about 400°C for both carbon contents. Contrary to fully dense steels, tempering above 500°C only slightly improved the impact resistance of sinter hardened materials.

5. The properties of sinter hardened materials can be tailored to application requirements:
   - A high combined carbon, such as 0.80%, without tempering is recommended to maximize apparent hardness. This is achieved to the detriment of the strength and impact resistance.
   - Tempering at 150°C using a high combined carbon material is a good compromise to maintain high apparent hardness with better strength and impact resistance.
   - The highest tensile strength and impact resistance are reached with a medium carbon material, 0.65% C, tempered 200°C.

REFERENCES

1. R. Ratzi, “Modern Methods for the Heat Treatment of High Strength Sintered Parts”, In-House P/M Seminar on Advanced P/M Components for the Automotive Industry, Adam Opel AG, EPMA, June 21, 1993.
2. H. Ferguson, “The Heat Treatment of P/M Steels-an Overview”, Proceedings of the 16th ASM Heat Treating Society Conference & Exposition, 19-21 March 1996, Cincinnati, OH.
3. W.F. Smith, “Structure and Properties of Engineering Alloys”, McGraw-Hill Book Company, N.Y., 1981, p.124-125.

4. H. Miura, T. Baba and T. Honda, "The Effect of Heterogeneous Structure on the Properties of Sintered Low Alloy Steels", Advances in Powder Metallurgy & Particulate Materials, Vol. 4, compiled by T.M. Cadle and K.S. Narasimhan, Metal Powder Industries Federation, Princeton, NJ, 1996, p. 13-42.
5. H. Danniger, D. Spoljaric, A. Arakil and B. Weiss, " Mo Alloyed PM Structural Steels prepared by Different Alloying Techniques", Advances in Powder Metallurgy & Particulate Materials, Vol. 4, compiled by T.M. Cadle and K.S. Narasimhan, Metal Powder Industries Federation, Princeton, NJ, 1996, p. 13-177.
6. R. Shivanath, P.K. Jones and R. Lawcock, "On the Synergies of High Temperature Sintering and Alloy Development for High Endurance P/M Powertrain Components", Advances in Powder Metallurgy & Particulate Materials, Vol. 4, compiled by T.M. Cadle and K.S. Narasimhan, Metal Powder Industries Federation, Princeton, NJ, 1996, p. 13-427.
7. H. Ferguson, G. L'Espérance, E. Duchesne and A.F. de Rege, "Effect of Mass/Cross Sectional Thickness on Sinter Hardened Steels of Different Hardenability", Advances in Powder Metallurgy & Particulate Materials, Vol. 2, compiled by R.A. McKotch and R. Webb, Metal Powder Industries Federation, Princeton, NJ, 1997, p. 14-67.
8. A.B. Davala, A.H. Graham and R.J. Causton, "Effect of Process Conditions Upon Sinter-Hardening Response of FLC-4608 Materials", Advances in Powder Metallurgy & Particulate Materials, Vol. 2, compiled by R.A. McKotch and R. Webb, Metal Powder Industries Federation, Princeton, NJ, 1997, p. 14-81.
9. F. Chagnon and D. Barrow, "Effect of Tempering Temperature on Sintered Properties of Sinter Hardened PM Steels", Advances in Structural PM Components Production, European Powder Metallurgy Association, Shrewsbury, UK, 1997, p. 273.
10. S.H. Avner, "Introduction to Physical Metallurgy", McGraw-Hill Book Company, NY, 1974, p. 256-260.
11. G. Krauss, "Steels: Heat Treatment and Processing Principles", ASM, Materials Park, OH, 1990, p. 43-106.
12. M. Gagné, Internal Report, 1996.
13. S.H. Avner, "Introduction to Physical Metallurgy", McGraw-Hill Book Company, NY, 1974, p. 305-313.
14. W.F. Smith, "Structure and Properties of Engineering Alloys", McGraw-Hill Book Company, N.Y., 1981, p. 62.
15. G. Krauss, "Steels: Heat Treatment and Processing Principles", ASM, Materials Park, OH, 1990, p. 205-261.
16. G. Krauss, "Steels: Heat Treatment and Processing Principles", ASM, Materials Park, OH, 1990, p. 145-178.
17. G. Krauss, "Steels: Heat Treatment and Processing Principles", ASM, Materials Park, OH, 1990, p. 1-16.